Ceramics International **23** (1997) 305–311

PII: S0272-8842(96)00023-5
0272-8842/97 $17.00 + 0.00

Sintering Behaviour of Sepiolite

A. A. Goktas, Z. Misirli & T. Baykara*

TUBITAK-Marmara Research Centre, Materials Research Department, P.O.B. 21, Gebze, Turkey

(Received 16 January 1996; accepted 25 January 1996)

Abstract: Sepiolite containing minerals from various regions of Turkey were processed to investigate their sintering behaviour over a wide temperature range. The sintering was studied by mercury porosimetry and nitrogen adsorption (BET). Microstructural features were investigated using SEM and TEM techniques. Physico-chemical and microstructural characterization of the sintered ceramic bodies demonstrated unusual pore structure (mean pore size of 0.02 micron within the range of 0.015–1.0 micron) retained even at temperatures as high as 1000 °C. A low linear shrinkage of 7.28% at 1100 °C indicates the potential promising applications in the field of filtering, molecular sieving and adsorption at higher temperatures. © 1997 Elsevier Science Limited and Techna S.r.l.

1 INTRODUCTION

Sepiolite is a hydrated magnesium silicate which consists of fibrous talc-like layers stacked in long ribbons with micro-channels and grooves parallel to the fibre axis. Based on such structural features and due to its high surface area along with the existence of a high physico-chemical activity, sepiolite is used in numerous applications such as filtering, adsorption, decolourization and molecular sieving. An ideal formula for sepiolite can be given as:

$$Si_{12}Mg_8O_{32}.nH_2O$$

It is shown that, on heating, the sepiolite structure loses bound water along with the loss of zeolitic water, resulting in tilting in the silicate layers (i.e. folding in the crystal) transforming the structure into a dehydrated form (sepiolite anhydride).[1,2]

Although, there have been a considerable number of studies on sepiolite devoted to structural analysis,[3–6] surface and adsorption characteristics,[7–9] dehydration behaviour,[10–14] rheological and catalytic properties[15–18] and other physico-chemical characteristics,[19–22] there is a considerable lack of information and data on the sintering of sepiolite base ceramic materials. The sintering behaviour of sepiolite can have interesting characteristics, since sepiolite is an unusual material which has structural features that may lead into further applications as a bulk ceramic material. In this regard, the purpose of the present study is to investigate the sintering behaviour along with the physical characteristics of the heated and unheated sepiolite samples. Microstructural features and physical properties of the sintered samples were also determined for the evaluation of the material's characteristics.

2 EXPERIMENTAL

Natural sepiolite samples of Eskisehir-Sivrihisar region were collected in as-received forms, crushed and ground into powdered form using 45 mesh sieves. Eskisehir-Sivrihisar, brown coloured sepiolite is denoted as Sepiolite A; Eskisehir-Sivrihisar, beige coloured sepiolite is denoted as Sepiolite B. The chemical analysis of both sepiolite samples determined by atomic absorption method are given in Table 1. As for the compositional features concerned, one should note that the sample A is sepiolitic-dolomitic, while the sample B can be considered as purely sepiolitic in nature. Particle size and distribution analysis of powdered samples using sedigraph indicates that 50% of Sepiolite A is under 2 micron in size, while 50% of Sepiolite B is under 4 micron in size.

*To whom correspondence should be addressed.

Powdered samples were then compacted uniaxially to a bar shaped form (0.4×0.4×4.0 cm) under 1 ton/cm^2 pressure. The surface area determinations using BET technique with nitrogen adsorption, porosity and density measurements using mercury porosimeter and picnometer, respectively, are tabulated for the powdered sepiolite samples in Table 2. The samples of Sepiolite A and B exhibit surface area values of 244 and 402 m^2/g, respectively. Porosity levels of the samples are found in the range of 47.6%–50.8%. The density values are measured to be 2.49–2.59 g/cm^3. Porosity measurements on green and sintered bodies were made to determine mean pore diameter and pore size distribution and are shown in Table 3. Samples were sintered over a wide temperature range of 300–1200 °C at a heating rate of 10 °C/min for 1 h sintering hold under normal furnace atmosphere and allowed to cool to room temperature in the furnace atmosphere. The weight loss and structural changes during heat treatment were determined by thermal gravimetric analysis (TGA) and differential thermal analysis (DTA). Other physical property measurements for the percent shrinkage after sintering, percent porosity, pore size and pore size distribution and three-point bending test were carried out on the sintered samples. X-ray and IR spectral analyses were also performed on as-received powders and the sintered samples. The microstructures of the as-received, compacted and sintered samples were studied by SEM and TEM techniques. TEM studies were made on the loose powders of as-received sepiolite samples. A very dilute solution of ground and sieved powders with 0.3% Formvar in chloroform was prepared, and small drops of this suspension were air dried on the carbon coated copper grids. The grids were then coated with ~200 Å carbon.

Table 1. Chemical analysis of the sepiolite samples

	Sepiolite A	Sepiolite B
SiO_2	51.80	64.80
MgO	28.40	23.20
CaO	12.60	1.16
Al_2O_3	1.63	4.35
FeO	0.69	1.76
TiO_2	0.06	0.19
K_2O	0.24	0.56
Loss of ignition	4.58	3.98

Table 2. Physical properties of the sepiolite samples

Physical property	Sepiolite A	Sepiolite B
Surface area (m^2/g)	244	402
Porosity (%)	50.8	47.6
Density (g/cm^3)	2.59	2.49

Table 3. Pore size range and mean pore size upon heating in the sepiolite samples (in micron)

Sepiolite sample	25 °C	900 °C	1000 °C
A	0.01–0.1	0.03–1.0	0.05–1.0
	0.023	0.15	0.13
B	0.015–0.1	0.01–0.03	0.015–4.0
	0.030	0.015	0.02

3 RESULTS AND DISCUSSION

DTA and TG analysis were employed to study the structural alteration of the sepiolite samples upon heating. DTA and TGA curves, which were recorded simultaneously with a heating rate of 10 °C/min, are shown in Fig. 1(a) and (b). DTA curves show structural alteration during the heat treatment

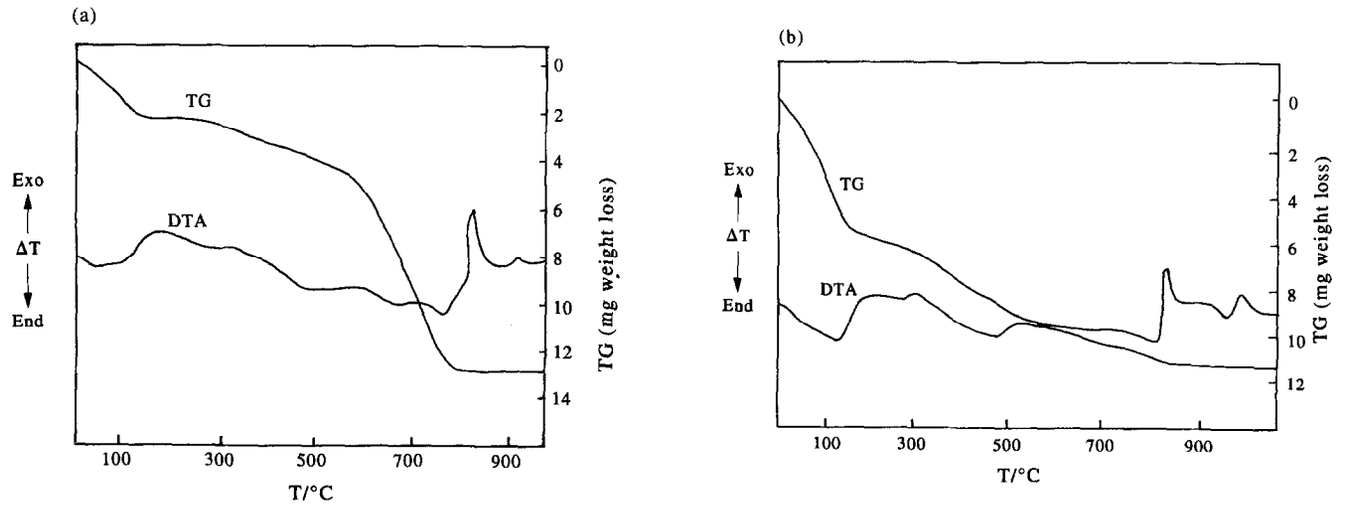

Fig. 1. DTA and TGA curves for the sepiolite samples: (a) sample A; (b) sample B.

Table 4. Crystallization products of the sepiolite samples upon heating (as determined by XRD analysis)

	Sepiolite A	Sepiolite B
25 °C and	Dolomite	Sepiolite
300 °C	Sepiolite	Dolomite
900 °C	Diopside Clinoenstatite	Clinoenstatite

of both sepiolite samples, exhibiting endothermic peaks at 65–120 °C which indicate the loss of zeolitic water, while endothermic peaks at 275–325 °C and 425–500 °C show two step removal process of coordinated water molecules. It should be noted that similar DTA curves for various sepiolite samples have been reported in some literature.[12,13] In the range of 775–830 °C, it is observed that a final endotherm is present, followed by distinct exothermic

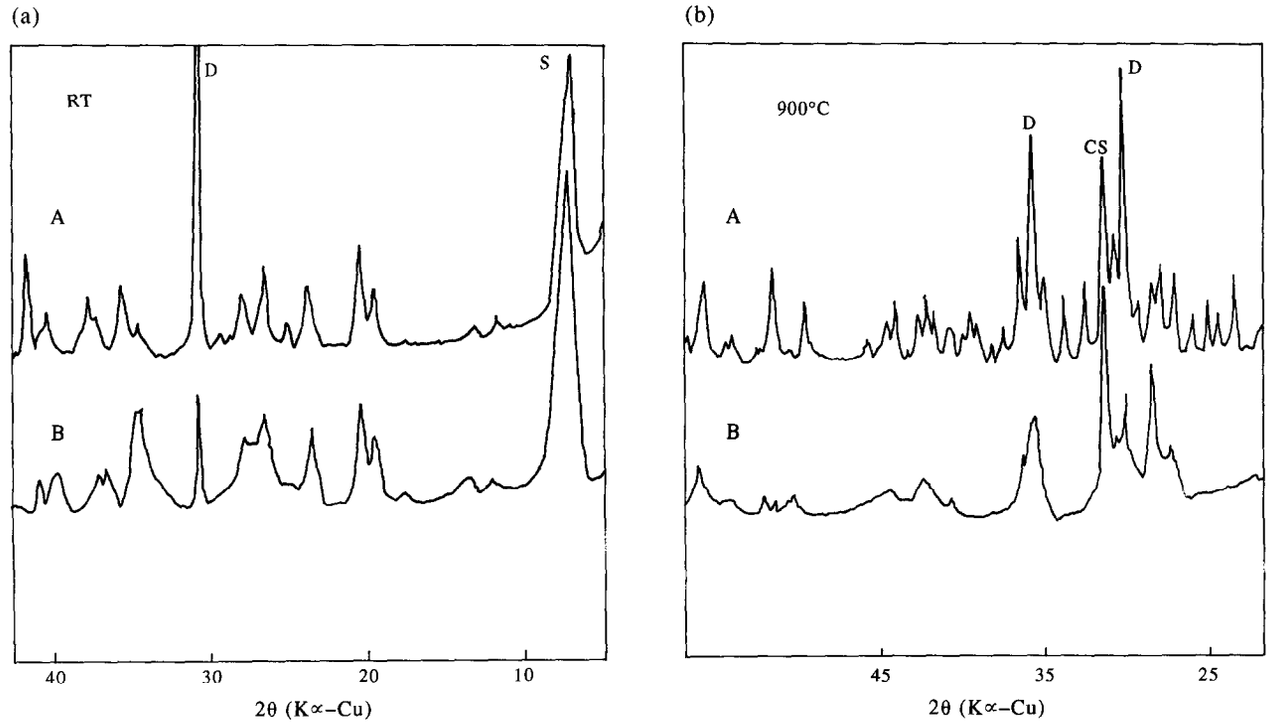

Fig. 2. XRD patterns of the sepiolite samples (a) at room temperature and (b) at 900 °C. A — Sepiolite A; B — Sepiolite B.

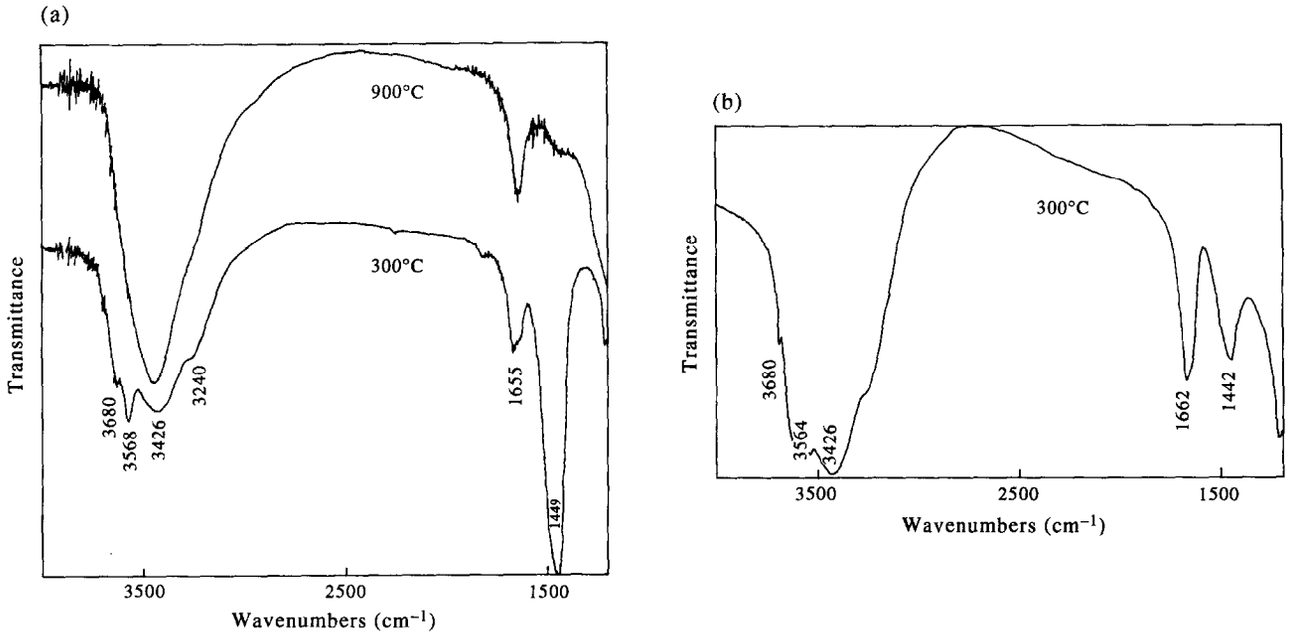

Fig. 3. The infrared spectra for the sepiolite samples: (a) sample A; (b) sample B.

peaks at 830–925 °C. The endothermic peak may be associated with the loss of hydroxyl groups, while the exotherms suggest the recrystallization of other modified structures which were also reported in the previous studies.[12,13]

TGA evaluation of the sepiolite samples consistent with the DTA data showed loss of the zeolitic and coordinated, bound water molecules and dehydroxylation of sepiolites during the heat treatment. The dehydration behaviour of samples A and B are comparable to those described in previous studies.[5,12,13] TGA curves given in Fig. 1(a) and (b), suggest that weight loss during heating caused by the removal of zeolitic water occurs at temperatures below 150 °C, while the loss of bound water molecules occurs in two steps at about 200–350 °C and 350–600 °C. The final weight loss at 600–800 °C is caused by dehydroxylation of the sepiolite samples. As can be seen in Fig. 1(b), the TGA curve for the Sepiolite B sample exhibits a more gradual weight loss behaviour after 350 °C compared with that of the Sepiolite A sample.

X-ray diffraction patterns for as-received powders and samples heated up to 1000 °C were analysed and phase identification was carried out. The results are tabulated in Table 4 and shown in Fig. 2(a) and (b). It should be noted that heating of the samples up to 350 °C did not change the XRD pattern reflections. Further heating of the samples up to 900 °C resulted in the recrystallization of the sepiolites into the new forms of clinoenstatite and diopside (Sepiolite A) and clinoenstatite (Sepiolite B).

Infrared spectroscopic analysis of unheated and heated sepiolites was achieved using KBr discs in the range of 4000–1200 cm^{-1}. The infrared spectra for the sepiolite samples heated at 300 and 900 °C are shown in Fig. 3(a) and (b). It was observed that the spectra for room temperature sepiolites were identical to those of the samples heated at 300 °C and therefore are not given here. All of the IR spectral curves show absorption bands located in the regions of 3425–3680 and 1630–1660 cm^{-1}, which are assigned to the hydroxyl stretching and molecular water deformation modes, respectively.[3,12] The bands observed at 3680 cm^{-1} correspond to the OH stretching vibration of the Mg–OH groups, while the bands at 3425 and 3240 cm^{-1} are attributed to the zeolitic water content. The spectral curve given in Fig. 3(a) also reveals the presence of a band at 1450 cm^{-1} in the low temperature spectra for sample A. This band disappears when the sample was heated to 600 °C suggesting the presence of organic groups. It is interesting to note that hydroxyl stretching absorption bands at 3425 and 3570 cm^{-1} can be identified for the sample sintered at 300 °C, while the band at 3425 cm^{-1} can still be identified for the sample sintered even at 900 °C. The stretching absorption bands of O–H belonging to zeolitic water at 3425 cm^{-1} for the sample sintered at

Table 5. % porosity level upon heating in the sepiolite samples

Sepiolite samples	25 °C	900 °C	1000 °C	1100 °C
A	50.8	54.0	52.6	49.9
B	47.6	55.0	41.4	12.0

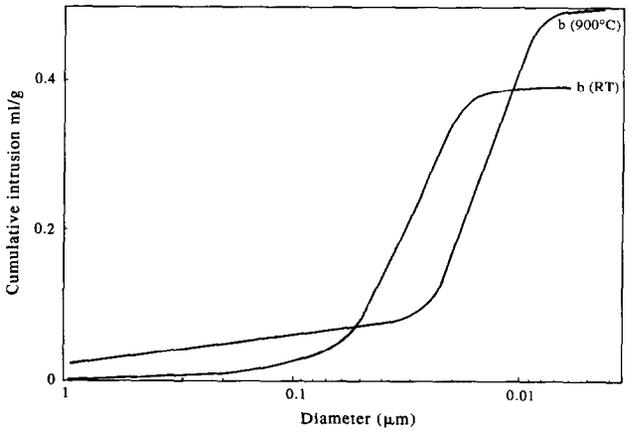

Fig. 4. Cumulative intrusion vs pore diameter for the sepiolite samples.

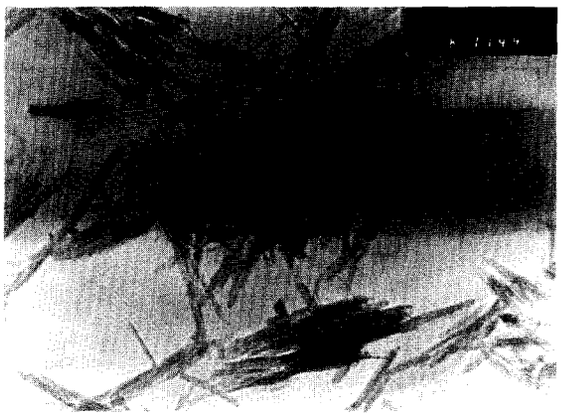

Fig. 5. A TEM photomicrograph of the Sepiolite A sample at room temperature, loose form ×16,000.

Table 6. Linear shrinkage (%) of the sepiolite samples as a function of temperature

Sepiolite samples	600 °C	900 °C	950 °C	1000 °C	1100 °C	1150 °C	1200 °C
A	0.71	4.42	4.89	6.60	7.28	15.8	17.9
B	0.71	5.97	8.50	16.5	—	—	27.6

300 °C seem to shift to 3450 cm^{-1} at 900 °C. The deformation bands appeared at 1630–1660 cm^{-1} associated with zeolitic and coordination water suggest that bound water molecules are still preserved and trapped within the structure of the sepiolite sample, even at 900 °C. Such a behaviour might be explained with internally tilted and collapsed channels which encounter diffusion and retard the escape of coordinated water from the crystal structure.[12]

The porosity conditions, such as the percent porosity, mean pore diameter and pore size distribution of the sintered samples, were characterized by mercury porosimetry. The results for the green samples and the samples sintered at 900, 1000 and 1100 °C are tabulated in Tables 3 and 5. It should be noted that both of the sepiolite samples sintered at 900 °C maintained 54–55% porosity level with mean pore diameter of 0.015–0.15 micron and pore size distribution in the range of 0.01–1 micron. Such an unusual pore structure has been kept stable even at 1100 °C for the Sepiolite A samples with 49.9% porosity. However, for the samples of Sepiolite B, a sharp pore closure occurs at 1100 °C reduced to 12%. Cumulative intrusion vs pore diameter for the green samples of Sepiolite B and the samples sintered at 900 °C are given in Fig. 4. The linear shrinkage data given in Table 6 also supports this unusual pore structure of the Sepiolite A samples, indicating maximum 7.28% shrinkage at 1100 °C. It is interesting to note that both samples exhibit low shrinkage rates up to 600 °C at the level of 0.70–1.43%.

Smooth, creamy white coloured appearance of the Sepiolite A samples sintered after 600 °C suggests a low impurity level in the structure. Three-point bend tests on sintered Sepiolite A samples resulted in strength values of 16, 47 and 85 kg/cm^2 sintered at 900, 1000 and 1100 °C, respectively.

The morphologies of the loose, as-received sepiolite powders were examined using TEM techniques.

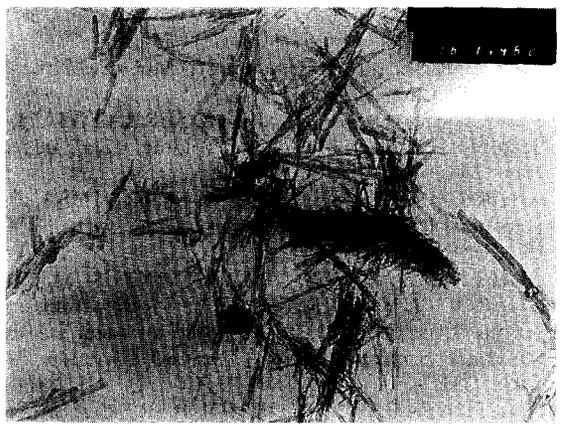

Fig. 6. A TEM photomicrograph of the Sepiolite B sample at room temperature, loose form ×16,000.

As apparent in the TEM micrograph given in Fig. 5, the Sepiolite A sample is composed of bundles of short sepiolite fibres of average 1.75 micron length and 0.5 micron width in size. Small dolomitic particles are located in between and at the edges of fibres. In Fig. 6, a TEM micrograph of the Sepiolite B sample is shown. Sepiolites of average 2.0 micron length and 0.3 micron width are distributed as fibre aggregates and individual fibres. The appearance of this fibrous structure indicates that these sepiolite samples may have a promising application in the field of filtering and molecular sieving.

Microstructural evaluation of the fractured surfaces was carried out using scanning electron microscopy techniques. Figure 7(a) shows an SEM-SEI (secondary electron image) photomicrograph of a fractured surface of the Sepiolite A sample sintered at 600 °C. Typical fine fibrous appearance of the structure can be seen in the sample. Large fracture holes and cracks in between the fibrous and fine granular structure can be observed in Fig. 7(b). In Fig. 8, a fractured surface of the Sepiolite A sample sintered at 950 °C is shown to demonstrate a very fine and loose granular appearance with microporosities. The effect on the fracture

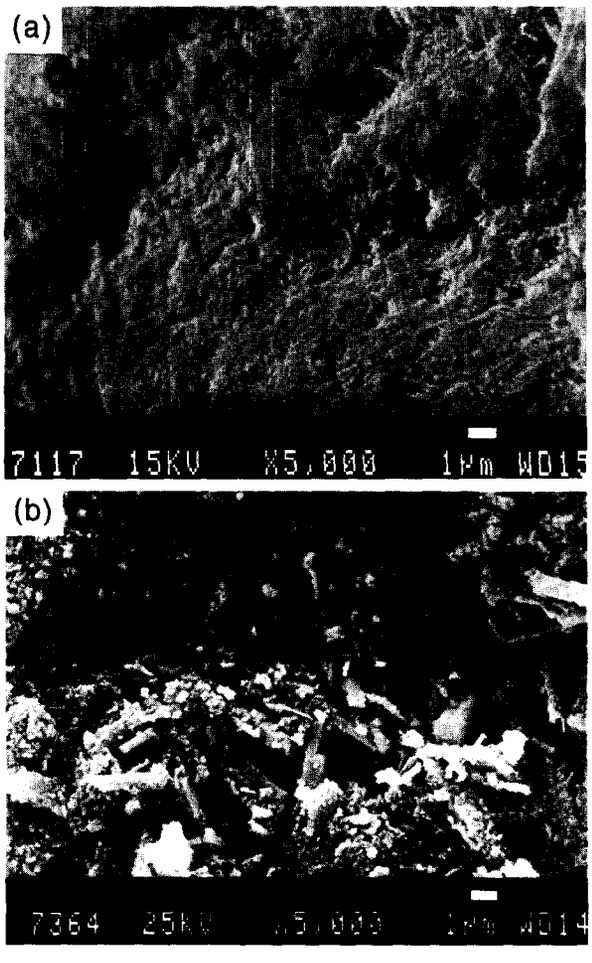

Fig. 7. SEM-SEI photomicrographs of a fractured surface of the Sepiolite A samples sintered at 600 °C.

surfaces of the Sepiolite A samples sintered at 1000 °C can be seen in Fig. 9(a) and (b). Particle size distribution and morphological features exhibit considerable differences in the microstructure. Hence, it might be suggested that the possible application of these samples in the field of filtering, molecular sieving and adsorption may have a limitation at that temperature range. Fine fibrous particles agglomerated loosely in a structure with continuous channels of 1 micron width [Fig. 9(a)], whereas in some other areas distinctly observed sintering is evident, as shown in Fig. 9(b) in which 1–2 micron size pores are regularly spaced and distributed throughout the structure.

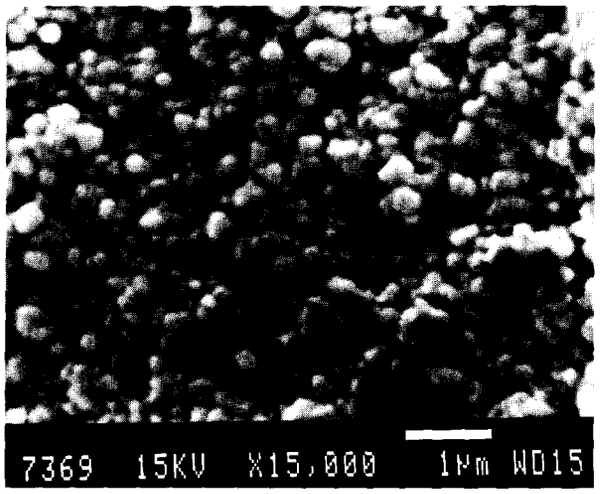

Fig. 8. A SEM-SEI photomicrograph of a fractured surface of the Sepiolite A sample sintered at 950 °C.

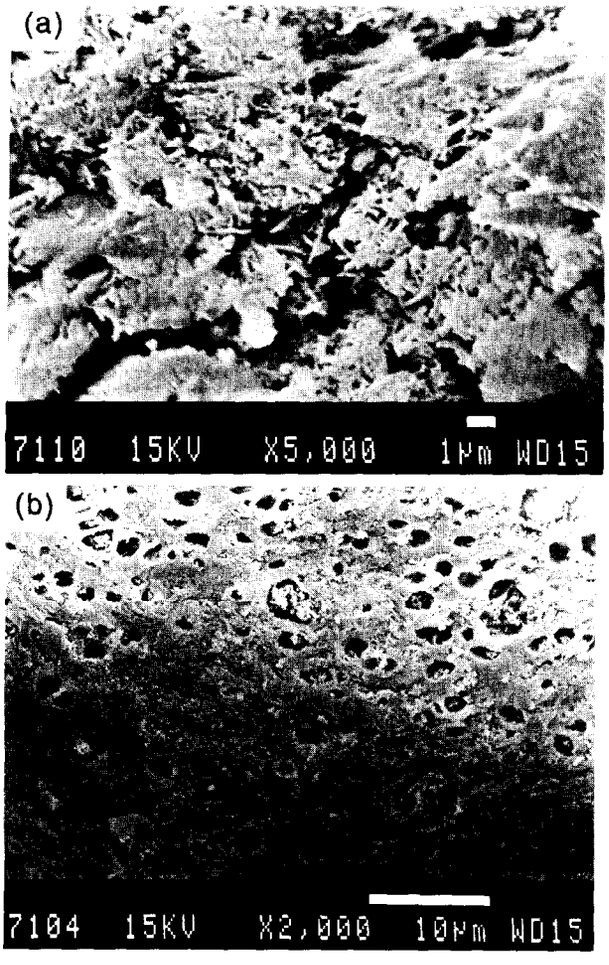

Fig. 9. SEM-SEI photomicrographs of a fractured surface of the Sepiolite A samples sintered at 1000 °C.

4 CONCLUSION

The present study investigated some of the physical and structural characteristics and the sintering behaviour of sepiolite samples from Eskisehir-Sivrihisar regions of Turkey. The IR spectra of the sepiolite samples provided information regarding the removal of zeolitic and bound water and organics. SEM and TEM micrographs revealed that the sepiolites have a fibrous structure consisting of flat laths joined together at their edges. Analysis of the structure demonstrated the porosity development with the mean pore size values around 0.02 micron in the pore size range of 0.015–1.0 micron retained at 1000 °C. A low linear shrinkage value of 7.28% was also determined at temperatures as high as 1100 °C. Such results and findings indicated that the sepiolite has a promising potential in high temperature applications due to its microporous and fibrous structure retained at temperatures as high as 1000 °C.

ACKNOWLEDGEMENT

The authors thank the General Directorate of Mineral Research and Exploration (MTA) of Turkey for supplying samples.

REFERENCES

1. BRAUNER, L. & PREISINGER, A., Struktur und entstehung des sepioliths. *Tschermaks. Min. Petr. Mitt.*, **6** (1956) 120–140.
2. GRIM, R. E., *Clay Mineralogy*. McGraw–Hill, New York, 1968, pp. 117–118.
3. SERNA, C., AHLRICHS, J. L. & SERRATOSA, J. M., Sepiolite anhydride and crystal folding. *Clays and Clay Min.*, **23** (1975) 411.
4. AHLRICHS, J. L., SERNA, C. & SERRATOSA, J. M., Structural hydroxyls in sepiolites. *Clays and Clay Min.*, **23** (1975) 119.
5. GRILLET, Y., CASES, J. M., FRANCOIS, M., ROUQUEROL, J. & POIRIER, J. E., Modification of the porous structure and surface area of sepiolite under vacuum thermal treatment. *Clays and Clay Min.*, **36**(3) (1988) 233.
6. RAUTUREAU, M. & TCHOUBAR, C., Structural analysis of sepiolite by selected area electron diffraction-relations with physico-chemical properties. *Clays and Clay Min.*, **24** (1976) 43.

7. SERNA, C. J. & VANSCOYOC, G. E., Infrared study of sepiolite and palygorskite surfaces. In *Proc. of the Int. Clay Conf.*, ed. M. M. Mortland & V. C. Farmer. Elsevier, Amsterdam, 1978, pp. 197–206.
8. RUBICA, E. H., Sorption of Ni, Zn and Cd on sepiolite. *Clay Min.*, **20** (1985) 525.
9. BONILLA, J. L., LOPEZ-GONZALEZ, J. de D., RAMIREZ-SAENS, A., RODRIGUEZ-REINOSO, F. & VALENZUELA-CALAHORRO, C., Activation of a sepiolite with dilute solutions of HNO_3 and subsequent heat treatments — II. Determination of surface acid centres. *Clay Min.*, **16** (1981) 173.
10. NATHAN, Y., Dehydration of palygorskite and sepiolite. In *Proc. Int. Clay Conf., V. 1*, Tokyo, Japan, 1969, p. 91.
11. IMAI, N., Dehydration of palygorskite and sepiolite from the Kuzuu district, Tochigi Pref., Central Japan. In *Proc. Int. Clay Conf., V. 1*, Tokyo, Japan, 1969, p. 99.
12. SERNA, C., AHLRICHS, J. L. & SERRATOSA, J. M., Folding in sepiolite crystals. *Clays and Clay Min.*, **23** (1975) 452.
13. NAGATA, H., SHIMODA, S. & SUDO, T., On dehydration of bound water of sepiolite. *Clays and Clay Min.*, **22** (1974) 285.
14. RAUTUREAU, M. & MIFSUD, A., Etude par microscope electronique des differents atats d'hydration de la sepiolite. *Clay Min.*, **12** (1977) 309.
15. SANTAREN, J., Sepiolite: A mineral thickener and rheology additive . *Modern Paint and Coatings*, **September** (1993) 68–72.
16. SIMONTON, T. C., KOMARNENI, S. & ROY, R., Gelling properties of sepiolite versus montmorillonite. *Appl. Clay Sci.*, **3** (1988) 165–176.
17. DANDY, A. J. & NADIYE-TABBIRUKA, M. S., Surface properties of sepiolite from Amboseli, Tanzania, and its catalytic activity for ethanol decomposition. *Clays and Clay Min.*, **30**(5) (1982) 347.
18. CORMA, A., PEREZ-PARIEN, J., FORNA, V. & MIFSUD, A., Surface acidity and catalytic activity of a modified sepiolite. *Clay Min.*, **19** (1984) 673.
19. CORMA, A., PEREZ-PARIENTE, J. & SORIA, J., Physico-chemical characterization of Cu-exchanged sepiolite. *Clay Min.*, **20** (1985) 467.
20. JIMENEZ-LOPEZ, A., LOPEZ-GONZALEZ, J. de D., RAMIREZ-SAENZ, A., RODRIGUEZ-REINOSO, F., VALENZUELA-CALAHORRO, C. & ZURITA-HERRERA, L., Evolution of surface area in a sepiolite as a function of acid and heat treatment. *Clay Min.*, **13** (1978) 375.
21. MIFSUD, A., CORMA, A. & GARCIA, I., Preparation of thermally stable sepiolite derivatives. *Mater. Lett.*, **6**(11/12) (1988) 436.
22. UEDA, H. & HAMAYOSHI, M., Sepiolite as a deodorant material: an ESR study of its properties. *J. Mater. Sci.*, **27** (1992) 4997–5002.